Available online at www.sciencedirect.com
ScienceDirect
Developmental Biology 300 (2006) 687–698
DEVELOPMENTAL BIOLOGY
www.elsevier.com/locate/ydbio

Cooperative Mesp activity is required for normal somitogenesis along the anterior–posterior axis

Mitsuru Morimoto [a], Makoto Kiso [a], Nobuo Sasaki [a], Yumiko Saga [a,b,*]

[a] *Division of Mammalian Development, National Institute of Genetics, Yata 1111, Mishima 411-8540, Japan*
[b] *SOKENDAI, Yata 1111, Mishima 411-8540, Japan*

Received for publication 20 March 2006; revised 10 July 2006; accepted 19 August 2006
Available online 24 August 2006

Abstract

Mesp2 is a bHLH-type transcription factor that plays a key role during somitogenesis. Mesp2 is transiently expressed and is quickly degraded once translated. In our current study, we find that Mesp2 contains a degradation domain, which acts as a target of proteasome-mediated proteolysis and appears to play this role in vivo. We have also defined the nuclear localization signals (NLS) and constructed a minimum Mesp2 protein (P2-HD) composed of the NLS, bHLH and the degradation domains. The ability of the P2-HD as a transcription factor in vivo was examined. Some of the defects that had been previously observed in the Mesp2-null mice were rescued in the knock-in mice but only in the posterior half of the body, indicating differential effects of P2-HD along the anterior–posterior (AP) axis. In addition, quantitative analysis of the expression along the AP axis revealed that the relative levels of *Mesp2* increased, whereas *Mesp1* is down-regulated in the later stages of development by the activities of Mesp2 in the wild-type embryo. Moreover, we have found that somitogenesis in the early stages is more susceptible to changes in the Mesp gene dosage, indicating that a threshold level of Mesp activity must be required for the progression of normal somitogenesis.

Keywords: Mesp1; Mesp2; Somitogenesis; Vertebra; Protein degradation; Proteasome; Knock-in mouse; Nuclear localization; Basic helix–loop–helix; Transcriptional factor

Introduction

Somitogenesis is a transient dynamic morphogenetic process that generates somites in a rostro-caudal progression by segmenting the paraxial mesoderm (Dubrulle and Pourquie, 2004). The somites provide basic axial structures that underlie the segmental architecture of not only the vertebra, ribs and muscles, which are all somite derivatives, but also of the vascular and nervous systems (Brand-Saberi and Christ, 2000; Monsoro-Burq and Le Douarin, 2000; Borycki and Emerson, 2000). The associated metamerism is regulated by periodic gene expression, that functions as a so-called segmentation clock in the presomitic mesoderm (PSM) in mouse (Aulehla and Johnson, 1999; Aulehla and Herrmann, 2004; Aulehla et al., 2003; Jouve et al., 2000; Bessho et al., 2001; Saga and Takeda, 2001; Giudicelli and Lewis, 2004). The periodicity is generated via a negative feed back loop of Notch signaling that activates the transcription of Hes7, which is a negative regulator of itself, and L-fng, which is a negative regulator of Notch signaling, and this results in the oscillation of Notch activity (Bessho et al., 2003; Rida et al., 2004). In addition, to achieve strict temporal control of the clock, the stabilities of both the mRNA and proteins have to be precisely regulated. Indeed, it has been shown that the Hes7 protein is actively degraded via an ubiquitin–proteasome pathway, which generates Hes7 protein oscillation in the PSM. Furthermore, somitogenesis is disrupted by the introduction of stabilized Hes7, in place of the wild-type protein. In knock-in mice, the periodic gene expression of both *Hes7* and *L-fng* is destroyed, which is consistent with the notion that stability of these proteins has to be precisely regulated in addition to their transcription and translation (Hirata et al., 2004).

We have been investigating the in vivo function of the bHLH transcription factor, Mesp2, for which the periodic expression of both mRNA and protein appears in the anterior PSM (Saga et al., 1997). Mesp2 defines the segmental border by suppressing Notch signaling via the activation of *L-fng* and the suppression of *Dll1*

* Corresponding author. Division of Mammalian Development, National Institute of Genetics, Yata 1111, Mishima 411-8540, Japan. Fax: +55 981 6828.
E-mail address: ysaga@lab.nig.ac.jp (Y. Saga).

0012-1606/$ - see front matter © 2006 Elsevier Inc. All rights reserved.
doi:10.1016/j.ydbio.2006.08.043

(Takahashi et al., 2000; Morimoto et al., 2005). Moreover, Mesp2 also defines the rostral identity of the somites by suppressing the expression of *Dll1* and *Uncx4.1*, which is required for the development of their caudal properties (Takahashi et al., 2003). Thus, Mesp2 plays key roles in the anterior PSM, at the point of transition of the paraxial mesodermal cells from the PSM to somites. In addition, we have previously shown that Mesp1 is a closely related member of the Mesp family of genes, which share significant sequence homology in their bHLH regions (Saga et al., 1997). These genes are co-expressed in the early mesoderm, just after gastrulation, and in the paraxial mesoderm during somitogenesis. They also show a good degree of functional redundancy, since a knock-in of Mesp1 into the Mesp2 locus can rescue most of the defects that are observed in the Mesp2-null mouse (Saga, 1998). However, the functions of Mesp1 and Mesp2 during somitogenesis are likely to be slightly different as chimeric analyses have revealed that Mesp1 contributes to the epithelialization of the somites but that Mesp2 is essential for establishing rostro-caudal patterning (Takahashi et al., 2005).

In our current study, we have attempted to define the functional domains of the Mesp2 protein by focusing on the vertebral development reflecting rostro-caudal properties of somites in vivo. After determining both the degradation domain and the nuclear localization signal of Mesp2, we constructed a possible minimum functional Mesp2 protein containing the conserved bHLH domain and assessed the ability of this truncated factor to function in vivo by generating a Mesp2 locus knock-in of the construct. The knock-in mice showed a hypomorphic phenotype in which the defects are confined within the anterior half of the axial skeleton. Comparative analyses of the expression of the Mesp family genes subsequently revealed that the relative levels of *Mesp1* and *Mesp2* change during somitogenesis, and that a compensatory increase in *Mesp1* may contribute to rescue events in the posterior half of the axial skeleton.

Material and methods

Plasmid construction

Various constructs of Mesp2 were generated according to standard molecular techniques. Deletion mutant constructs were created by PCR-mediated methods, followed by ligation to native flanking DNA fragments. The wild-type and deletion mutants were cloned into the p3xFLAG-CMV vector (Sigma). EGFP-tagged Mesp2 variants were generated by inserting the Mesp2 coding sequence between EGFP and the poly-A signal.

Expression experiments using cultured cells

COS7 and NIH3T3 cells were maintained in Dulbecco's modified Eagle's medium (DMEM) supplemented with 10% fetal bovine serum (FBS). Cells were transfected with 3xFLAG-Mesp2 wild-type or mutant constructs using FuGene 6 (Roche) according to the manufacturer's instructions. The cells were harvested 24 h after transfection and equal numbers of cells were replated with or without cycloheximide (30 μg/ml) and with the protease inhibitors, MG132 (50 μM), Z-Leu-Leu-Z (50 μM), PMSF (1 mM) or Pepstatin A (50 μM).

Immunoblotting of 3xFLAG-Mesp2 proteins in vivo

Western blot analysis was conducted using standard procedures. The PSM region of five embryos of each genotype was collected from same litters at E10.5. The samples were lysed in buffer containing 50 mM Tris (pH 7.4), 0.2 M NaCl, 1% Nonidet P40, 0.1% deoxycholate and a protease inhibitor cocktail (Roche). The tissue extracts were separated by SDS-PAGE on 7.5% gels. The 3xFLAG-Mesp2 signals were detected by anti-FLAG antibody F3165 (Sigma) and quantified using NIH Image. The signals were normalized to the expression levels of β-actin which were detected by anti-β-actin antibody A2066 (Sigma).

Gene knock-in strategy

To generate several knock-in vectors for Mesp2 variants, we initially constructed a targeting vector cassette with the gateway system (Invitrogen), in which attL1 and attL2 were included in the site where the Mesp2-cDNA variants to be inserted. The Mesp2 cDNAs (P2-full, P2-ΔD, P2-HD) were subcloned into the entry vectors for the gateway system and the final constructs were generated by in vitro homologous recombination (Supplementary Fig. S1). Introduction of the targeting vectors into ES cells (TT2) and subsequent screenings were conducted as previously described (Yagi et al., 1993; Kitajima et al., 2000). The chimeric mice were then crossed with ICR female mice to establish each mouse line.

Histology, histochemistry and gene expression analysis

Section in situ hybridization and immunohistochemical detection of proteins were performed as previously described (Morimoto et al., 2005). The methods used for gene expression analysis by in situ hybridization of whole-mount samples and skeletal staining have been described previously (Saga et al., 1997; Takahashi et al., 2000).

Real-time PCR

Three primer pairs, one specific for *Mesp1*, one for *Mesp2* and *G3PDH*, were designed: Mesp1-L1 (5′-CCTTCGGAGGGAGTAGATC-3′) and Mesp1-R1 (5′-AAAGCTTGTGCCTGCTTCA-3′); Mesp2-L2 (5′-GACTGGACACTGGACACAATCCACT-3′) and Mesp2-R2 (5′-GGCCATAGCCAAGCAGACCTCAAA-3′); G3PDH-Fw (5′-ACCACAGTCCATGCCATCAC-3′) and G3PDH-Rv (5′-TCCACCACCCTGTTGCTGTA-3′). The housekeeping *G3PDH* gene was used as "reference" gene. PCR reactions were carried out in 48-well microtiter plate wells in a 20 μl reaction volume with SYBR premix Ex Taq (TAKARA) with optimized concentrations of specific primers. An BIO-RAD MiniOpticon Real Time PCR Detection System (BIO-RAD) was programmed for an initial step of 10 s at 94°C, followed by 39 thermal cycles of 15 s at 94°C, 15 s at 60°C, 30 s at 72°C. Every assay was run in triplicate and negative controls (no template, template produced with no RT enzyme) were always included. For each sample 1 μg of total RNA was reverse transcribed. A 1:25 dilution of each cDNA was used as template in real-time PCR. Specificity of PCR amplification of each primer pair was confirmed by melting curve analysis (Ririe et al., 1997). Standard curves were generated by measuring threshold cycle (CT) values of ten-fold serial dilutions of the calibrator cDNAs for *Mesp1* and *Mesp2*. The relative transcript level was determined by a method and formula as described (Pfaffl, 2001). To compare the level of *Mesp1* expression in different genotypes, embryos were collected and pooled after genotyping. *Mesp1* expression level of each sample was normalized against G3PDH. For the measurement of relative expression levels between *Mesp1* and *Mesp2*, three independent embryo samples were prepared from different stages and the value of *Mesp2* was normalized against *Mesp1*.

Results

A mechanism to destabilize Mesp2 protein

A striking feature of the Mesp2 protein is its restricted expression pattern in the anterior PSM every 2 h during somitogenesis. Since the Mesp2 levels quickly dissipate once the segmental border is established, we speculated that there must be specific mechanisms that destabilize the protein. To

elucidate these possible mechanism(s), we examined the stability of Flag-tagged Mesp2 protein, expressed in COS7 cells, with a number of protein inhibitors. Mesp2 protein is detectable as several bands, due to phosphorylation by endogenous kinases (Fig. 1 and Supplementary Fig. S2), and appears to be stabilized in the presence of MG132 (proteasome inhibitor), but not by Z-Leu-Leu-H, PMSF or Pepstatin A (a calpain, serine protease or aspartic protease inhibitors, respectively). To confirm this observation, a chase experiment was conducted in the presence of cycloheximide, in which the half life of Mesp2 protein was determined to be approximately 1.3 h in COS7 cells. The degradation rate, however, was remarkably inhibited in the presence of MG132, whereby the half life was extended to more than 4 h (Fig. 1B). These results indicate that Mesp2 is mainly degraded by the proteasome pathway, but also suggests the involvement of another mechanism because the complete inhibition of Mesp2 degradation was not achieved by MG132 treatment (Fig. 1B).

To identify the Mesp2 domain required for its degradation, a series of deletion mutants were individually expressed in COS7 cells and assayed for stability (Fig. 1C). A Δ311–330 mutant was found to be the most stable in our assay system and subsequent deletion analysis revealed that the region containing amino acids 326–330 is the most likely to confer sensitivity to the proteasome. We have thus designated this motif as the "degradation domain". To compare the effects of MG132 upon full-length and mutant Mesp2 (Δ311–330) in cultured cells, the protein levels were visualized by immunoblotting in the presence of either MG132 or DMSO (Fig. 1D). The Δ311–330 mutant protein was found to accumulate even in the absence of MG132, indicating that it is stabilized by its resistance to the proteasome pathway.

To confirm the destabilizing effect of the degradation domain of Mesp2 in vivo, we generated knock-in mice expressing FLAG-tagged -Mesp2 Δ326–330 (F-Mesp2ΔD) (Fig. 2A) instead of the wild-type protein (Supplementary Fig. S2). As a control, we also generated a knock-in mouse expressing FLAG-tagged full-length-Mesp2 (F-Mesp2-full). The heterozygous mice showed no abnormalities and the homozygous mice were also fertile in the cases of both F-Mesp2ΔD and F-Mesp2-full. To assess the stability of the introduced proteins, the neighboring sections of the PSM region were subjected to in situ hybridization analysis for *Mesp2* transcripts and immunohistochemical detection of Mesp2 protein. We found that the localization of the knock-in Mesp2 was similar to wild type (Fig. 2B). Unexpectedly, however, the mRNA expression levels of the introduced *Mesp2s* (both full-length and mutant) were lower than wild type (Fig. 2B). Since Mesp2 expression levels change cyclically during somitogenesis, we prepared several repeat samples and confirmed this lower transcription result. The reason for this effect is not clear but may be due to the unrelated nucleotide sequences in the 5′-untranslated region of the introduced by targeting vectors.

The level of protein expression was therefore also reduced in the knock-in mouse embryos and we noticed a broad expression domain for F-Mesp2ΔD. To determine the effects of a lack of the Mesp2 degradation domain in vivo, the protein expression levels were compared by anti-FLAG Western blot analysis using 5 tails from homozygous F-Mesp2ΔD and F-Mesp2-full E10.5 embryos (Fig. 2C). The subsequent results indicated that the F-Mesp2ΔD protein appears to be stabilized by the lack of a degradation domain in vivo, since these protein levels are relatively higher than F-Mesp2. In addition, comparative analyses of the skeletal specimens at E17.5 suggest that the degradation domain might be functional in vivo. The homozygous F-Mesp2-full mouse shows a fused rib phenotype at a high frequency (Fig. 2D). Interestingly, however, the F-Mesp2ΔD fetus shows this rib defect at lower frequency. We speculate that this situation may reflect the estimated lower production of F-Mesp2-full under knock-in conditions and that the defect is rescued by the stabilized F-Mesp2ΔD. To further confirm this rescue effect, we reduced the gene dosage by crossing F-Mesp2-full or F-Mesp2ΔD with Mesp1/Mesp2 double KO (dKO) mice and compared the skeletal phenotype in the presence of a single knock-in allele. The homozygous dKO mice die before E9.5 due to the lack of embryonic mesoderm (Kitajima et al., 2000) but the heterozygous mouse has no abnormality in the skeletal morphology (no rib fusion was detected among 6 fetuses examined). F-Mesp2-full/dKO embryos showed more severe abnormalities in the ribs and vertebra, with an average number of fused ribs of 16, whereas the average number of fused ribs was 6.5 in the F-Mesp2ΔD/dKO mice (Fig. 2D). These results indicate that the stability of F-Mesp2 ΔD may positively affect the function of Mesp2 and result in the suppression of the defect caused by a lower dosage of Mesp alleles.

Generation of a minimum functional Mesp2 protein

Mesp2 localizes to the nucleus in a cell as a transcription factor. To identify the minimum regions of Mesp2 that are required for a functioning protein, we screened for a putative nuclear localization signal (NLS) of Mesp2. Two arginine clusters (R70,71,73 and R145–150) that could be implicated as a potential NLS were identified outside of the basic helix–loop–helix (bHLH) domain. We replaced these amino acids with alanine residues and generated EGFP-tagged Mesp2 variants (Supplementary Fig. S3A). The cellular localization of the resulting Mesp2 proteins was then examined using confocal microscopy (Supplementary Fig. S3B). Wild-type Mesp2-EGFP was found to localize in the nucleus as expected, but the R70,71,73A and R145–150A variants were observed not only in the nucleus but also in the cytoplasm. Furthermore, the R70,71,73,145–150A variant was in fact mainly localized in the cytoplasm. We confirmed that these GFP fusion proteins were expressed as the correct size in the culture cells by the Western blotting (Supplementary Fig. S3B). These data suggest that R70,71,73 and R145–150 function as an NLS in the Mesp2 protein.

In addition to the degradation domain and the NLS, the bHLH domain is known to be required for DNA binding and for homo- or heterodimer formation. Hence, we tried to construct a minimal but functional Mesp2 (P2-HD protein) by combining the 3xFLAG tag with the regions 61–160aa

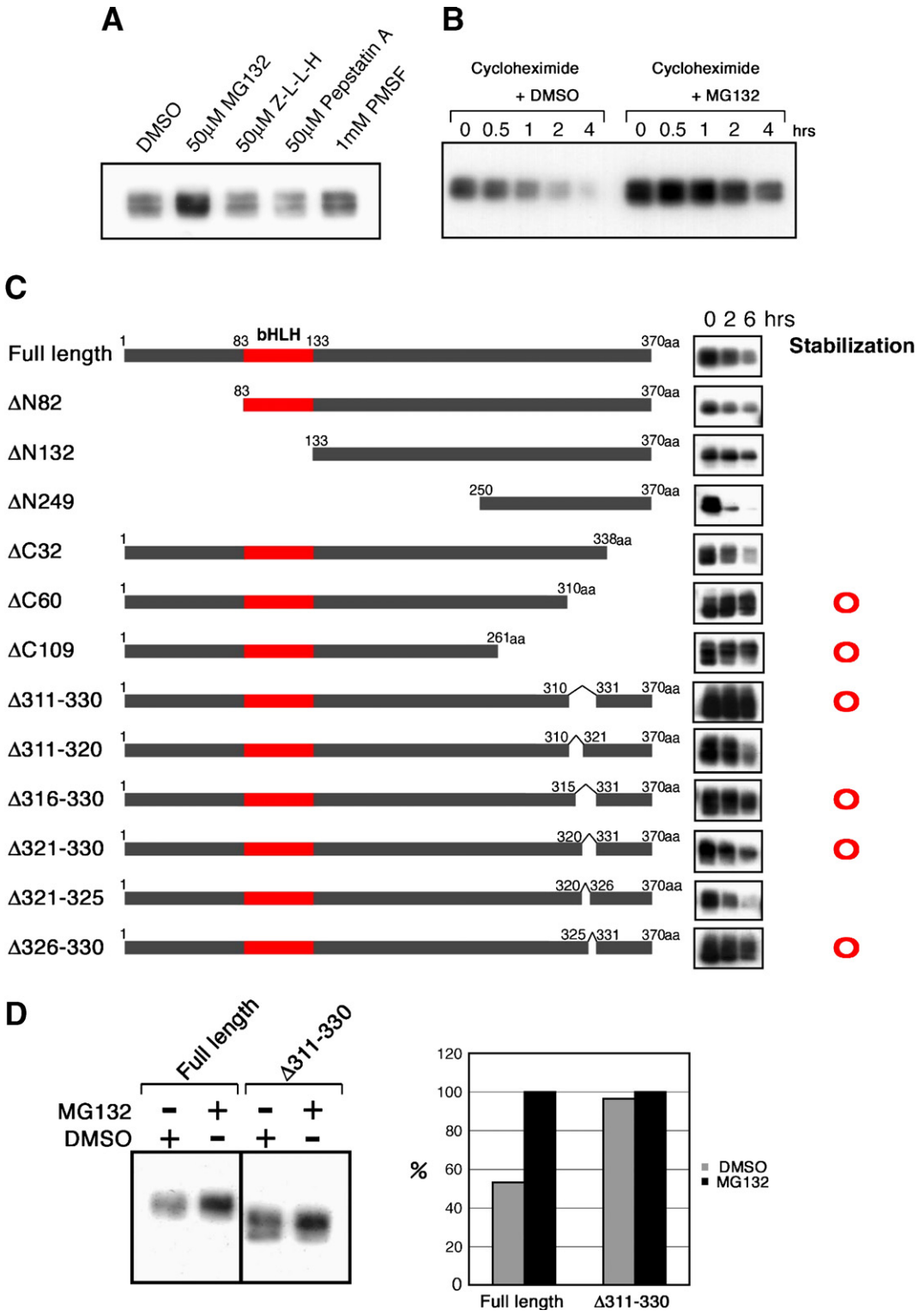

Fig. 1. The Mesp2 protein is degraded by the proteasome via its "degradation domain". (A) Cos7 cells transfected with 3xFLAG-Mesp2 (F-Mesp2) were incubated in the presence of cycloheximide and protease inhibitors, MG132, Z-L-L-H, PMSF or Pepstatin A for 2 h. The targets of these inhibitors are the proteasome, calpain, serine proteases and aspartic proteases, respectively. The F-Mesp2 proteins were detected by immunoblotting with anti-FLAG antibodies. (B) F-Mesp2 protein stability was analyzed in the presence of cycloheximide by treatment with either DMSO or MG132. The degradation process was then monitored by immunoblotting with anti-FLAG antibodies and was found to be inhibited by MG132 but not DMSO (vehicle control). (C) Functional mapping of the degradation domain of Mesp2. The degradation process was compared among the Mesp2 mutants shown in the figure by the same method used in panel B to identify the domains required for the degradation of Mesp2. Stabilized mutants are indicated by the red circles on the right. (D) Either full-length or D311–330 mutant F-Mesp2 was transfected into Cos7 cells and cultivated for 6 h with or without MG132. F-Mesp2 proteins were then detected by Western blotting (left panel) and quantified using NIH Image software (right panel).

(b*H*LH and NLS) and 311–338aa (*D*egradation domain) of Mesp2 (Supplementary Fig. S3C). We confirmed that this protein localized to the nucleus (Supplementary Fig. S3C). To investigate the function of the P2-HD in vivo, we then generated a P2-HD knock-in mouse using a similar method to that described in Supplementary Fig. S1. P2-HD heterozygous mice showed completely normal metameric vertebrae at E17.5 (Fig. 3A upper). In contrast, the P2-HD homozygous mice exhibited skeletal defects in the anterior region of the vertebra along the A–P axis, the cervical and thoracic vertebrae, and the rib (Fig. 3A middle). However, this phenotype was much milder than that of GFP-KI mice (Mesp2-null mice), in which the pedicles of the neural arches in the entire vertebra and the ribs are fused to each other as a result of the caudalization of somites, as shown previously (Fig. 3A lower, Takahashi et al., 2005). These data suggest that the P2-HD protein partially rescues the skeletal defects observed in the Mesp2-null mouse.

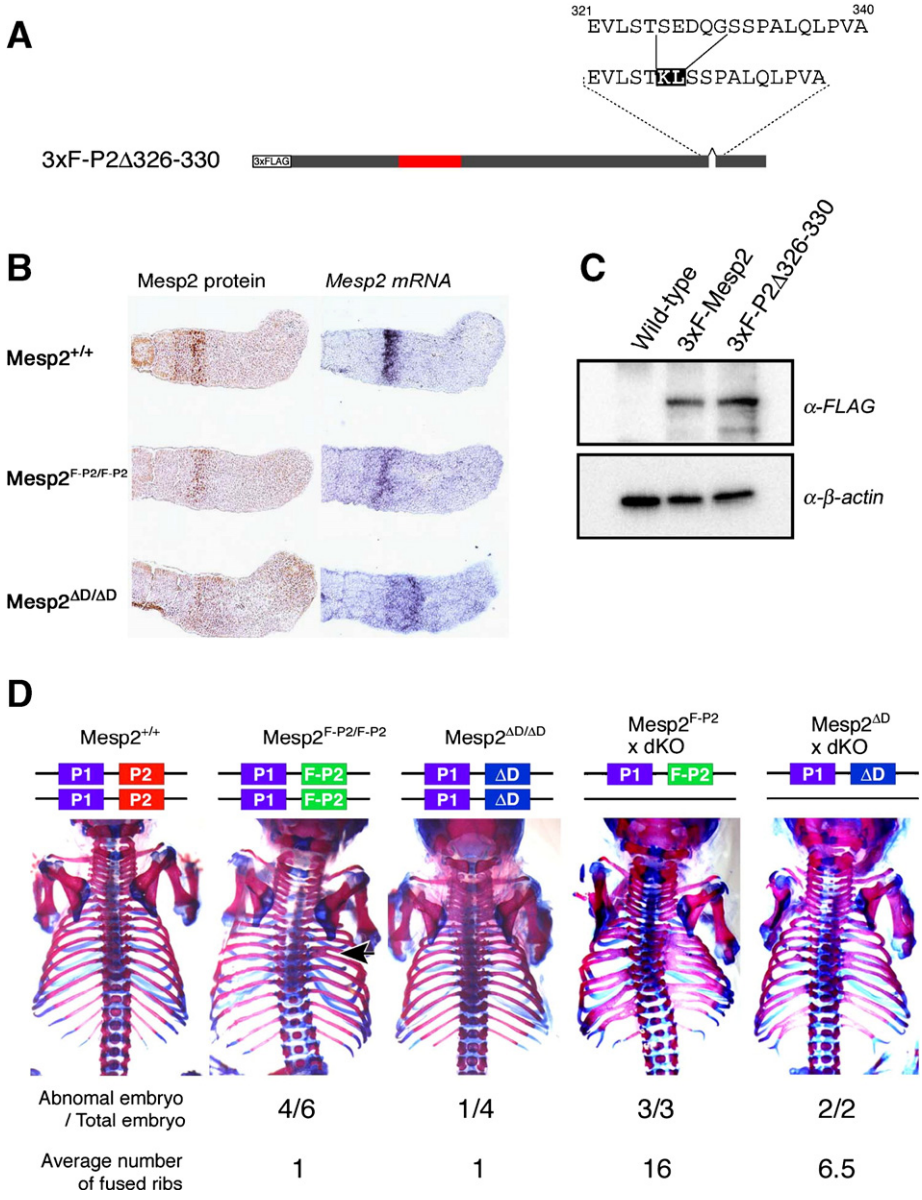

Fig. 2. A Mesp2 mutant protein that lacks the degradation domain is stabilized in vivo. (A) Schematic representation of a 3xFLAG-Mesp2Δ326–330 mutant (F-Mesp2 ΔD). (B) Comparison of the Mesp2 expression levels (protein and mRNA) among wild-type (WT) Mesp2, F-Mesp2 and F-Mesp2ΔD. Neighboring sections were subjected to detection by either anti-Mesp2 antibodies or RNA probes. Among specimens examined, representative samples containing the highest signals are shown. (C) Western blot analysis of Mesp2 proteins in vivo. Sample lysates were prepared from five PSM tissues of WT, F-Mesp2 or F-Mesp2ΔD embryos at E11.0 and Mesp2 proteins were then detected using anti-FLAG antibodies. Wild-type embryos served as a negative control (we have never successfully detected endogenous Mesp2 protein with anti-Mesp2 antibodies). The signal intensities were quantified using NIH Image and normalized to the expression levels of β-actin. (D) Comparative analyses of skeletal defects among different Mesp genotypes. The skeletal specimens were prepared at E17.5 and the defects observed in the rib were quantified by determining the number of fused sites. No fusions were detectable in the wild-type specimens. Fused ribs were detected in the homozygous F-Mesp2 mice at a higher frequency than in the homozygous F-Mesp2ΔD mice. A much more severe skeletal phenotype was observed in both the F-Mesp2/dKO and F-Mesp2ΔD/dKO embryos due to the lower Mesp dosage.

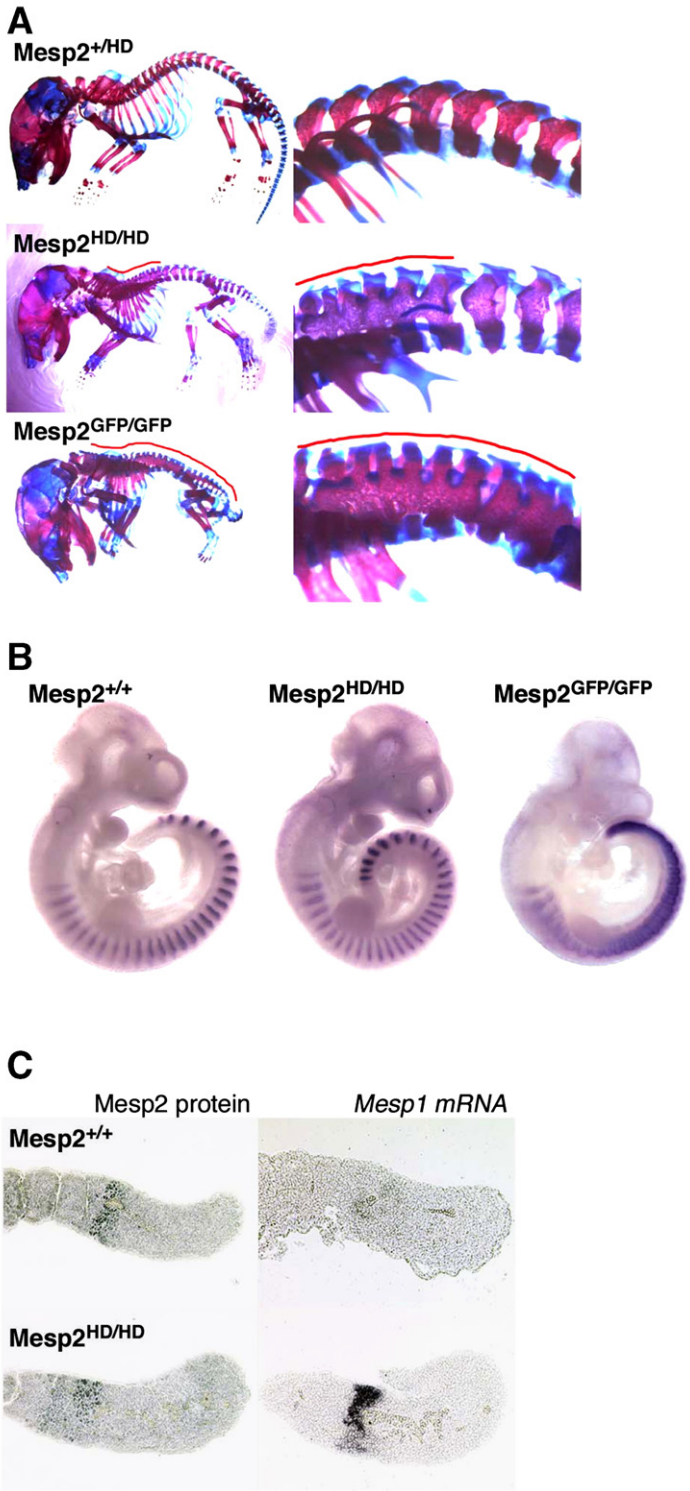

Fig. 3. The phenotype of a minimum Mesp2 functional mutant, P2-HD. (A–C) Comparative analyses of the skeletal morphologies at E17.5 (A) and the expression of *Uncx4.1* at E9.5 (B) in wild-type, P2-HD-KI or GFP-KI mice. (A) The homozygous P2-HD knock-in mouse exhibits skeletal defects in the anterior part of the axial skeleton, the cervical and thoracic vertebra and in the rib (middle panels in A). Much stronger defects are observed in the GFP-KI (Mesp2-null) mouse. Red lines indicate the skeletal defect region. (B) Metameric expression pattern of *Uncx4.1* is disrupted in Mesp2-null embryo (right panel). This abnormal expression is rescued in the homozygous P2-HD knock-in mouse (middle panel). (C) *Mesp1* expression is increased in the P2-HD embryo at E10.5. The expression levels of the P2-HD protein are lower than that of the wild-type (left panels). In contrast, the expression levels of *Mesp1* were found to be up-regulated in the P2-HD KI embryo (middle panels).

The expression of *Uncx4.1*, a caudal somite marker gene (Mansouri et al., 1997), was observed in the caudal compartments of the somites of both wild-type and P2-HD embryos, whereas an extended expression pattern was observed in the Mesp2-null embryo due to the lack of the rostral properties of the somites (Fig. 3B). Therefore, judging by the expression pattern of *Uncx4.1*, the minimal Mesp2 protein, P2-HD, can substitute for Mesp2 in vivo. However, the expression of P2-HD may not be sufficient to facilitate the gene regulation required during subsequent vertebral development, particularly in the anterior part of the axial skeleton. To determine the mechanism underlying this region-specific defect, we first analyzed Mesp2 expression using specific antibodies and found that the levels of P2-HD protein are lower than wild type (Fig. 3C). This phenomenon is consistent with our analyses of F-Mesp2 and Mesp2ΔD KI mice, which showed lower expression of both protein and mRNA for these species. On the other hand, using neighboring sections we have observed an up-regulation of *Mesp1* in the P2-HD homozygotes (Fig. 3C). In the GFP-KI homozygous embryo, *Mesp1* expression was also enhanced (Supplementary Fig. S4A). Since we have found that *Mesp1* expression is enhanced, and that Mesp1 also plays an important role in somitogenesis when the Mesp2 gene is defective (Takahashi et al. manuscript in preparation), we

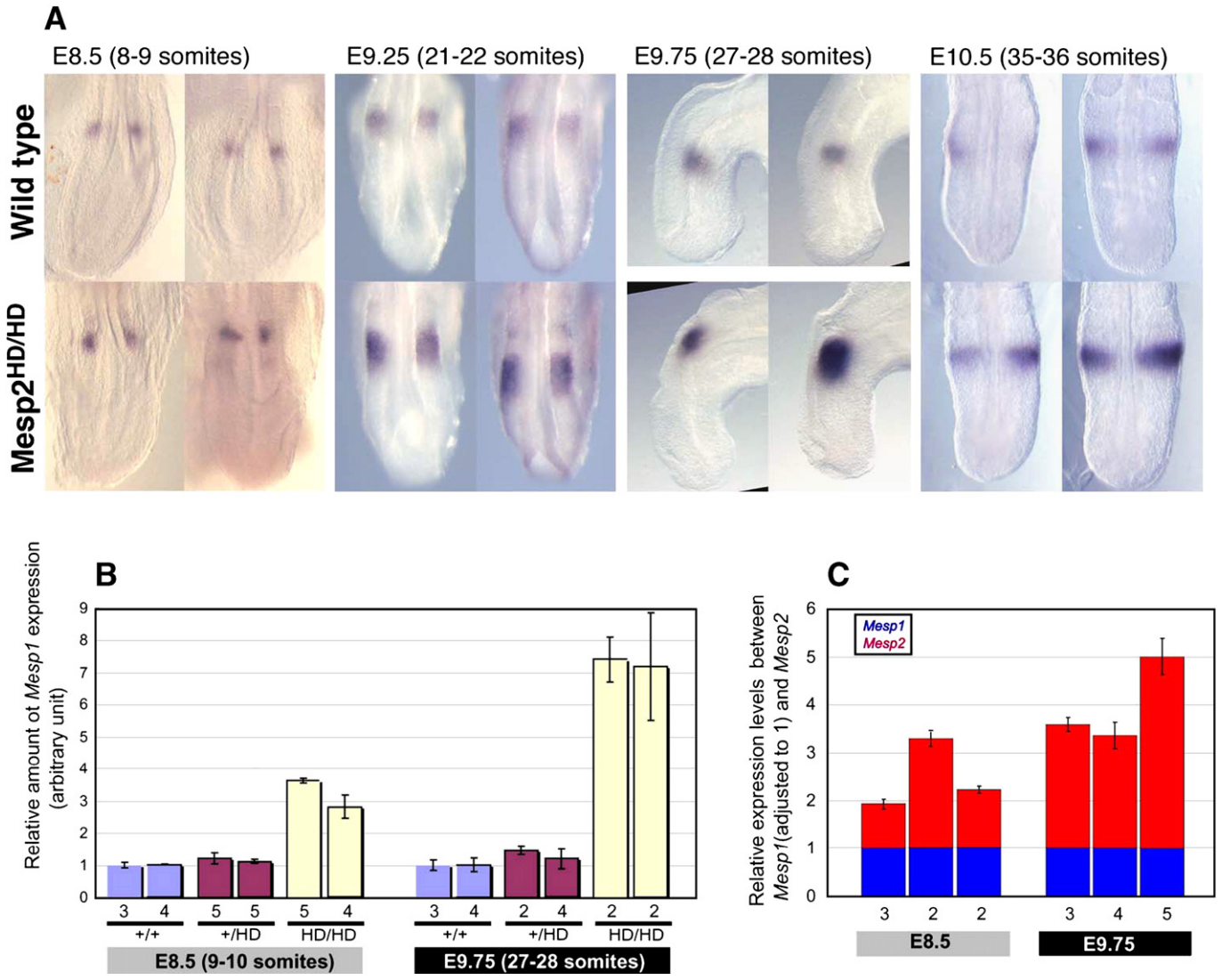

Fig. 4. The *Mesp1* expression levels increase as somitogenesis progresses in P2-HD KI mice. (A) Whole-mount in situ hybridization was performed with *Mesp1* probes using early (8 somites) to late (36 somites) somite-stage embryos. The *Mesp1* expression profile in the P2-HD KI embryo is stronger than wild type throughout somitogenesis. (B) The levels of *Mesp1* expression were compared among wild-type (+/+), P2HD heterozygous (+/HD) and P2HD homozygous (HD/HD) embryos using samples derived from two litters at two different developmental stages (E8.5 and E9.75). Total RNA isolates were prepared from pooled whole embryos and real-time PCR analysis was then conducted for each genotype. The numbers of embryos used in the analyses varied from 2 to 5 as indicated in the panel. The level of *Mesp1* mRNA was normalized to G3PDH. (C) The relative ratio of the *Mesp2* expression levels to that of *Mesp1* were examined at the early (E8.5) and later (E9.75) somite stages by real-time PCR with three different sets of cDNAs derived form wild-type embryos. These data were normalized to the levels of *Mesp1* expression. The numbers of embryos used were indicated in the panel.

hypothesized that the relative contributions of Mesp1 and Mesp2 might be regulated during somitogenesis and the region-specific defect that we observed in these experiments might reflect such a functional bias.

Differential expression of Mesp1 and Mesp2 during somitogenesis

Mesp1 and Mesp2 are transiently expressed prior to segmental border formation. Therefore, the downstream target genes must be involved in the subsequent chondrogenesis pathways that are required for skeletal development (Takahashi et al., 2000). Somites are sequentially generated from a rostral to a caudal direction and it is known that their regional specificity is defined when each somite is generated during development. Cervical vertebra are derived from 5–12 somites generated during E8.0–8.5, thoracic vertebrae are generated from 12–25 somites at E8.5–9.5, the lumbar are produced from 25–31 somites at E9.5–10.0, the sacral types are derived from 31–36 somites at E10.0–10.5 and caudal vertebrae are formed from 36–65 somites at E10.5–13.5 (Gossler and Tam, 2002).

To elucidate the contribution of Mesp1 to somitogenesis, and the reason why the P2-HD proteins show region-specific defects in the axial skeleton, the expression pattern of *Mesp1* was examined by whole-mount in situ hybridization from E8.5 (8–9 somites, cervical level) to E10.5 (35–36 somites, caudal vertebral level) (Fig. 4A). In P2-HD homozygous embryos, the expression level of *Mesp1* was found to be higher than that of the wild-type embryos throughout each of the stages examined. In addition, it appears that the level of *Mesp1* expression increases in the P2-HD embryo at the later stages, whereas it was relatively constant in wild-type embryos. We therefore reasoned that the normal vertebral formation from the posterior to the lumbar levels is probably due to the up-regulation of *Mesp1* during somitogenesis. To confirm this observation, we used quantitative RT-PCR to compare the levels of *Mesp1* during somitogenesis among wild-type and P2-HD hetero- or homozygous littermates at E8.5 and E9.75 (Fig. 4B). Since the embryo size differs from stage to stage, only the ratio among different genotypes was compared. At E8.5, *Mesp1* expression in P2-HD homozygous embryo was about 3.2-fold higher than wild type. At E9.75, this higher level of *Mesp1* was increased to about 7.6 fold above wild type. As previously reported, both Mesp1 and Mesp2 are expressed in the early nascent mesoderm but the expression is transient and become confined in the paraxial mesoderm after E8.25 just before somitogenesis (Saga et al., 1999). These data indicate that the differences in the expression levels of *Mesp1* between wild-type and P2-HD embryos increase with the progression of somitogenesis.

Since Mesp1 and Mesp2 have some similar functions, and the expression levels of both *Mesp2* and *Mesp1* are likely to be important, we next analyzed the relative expression levels of both genes using real-time PCR analysis with cDNAs from the wild-type embryos. Because both the *Mesp1* and *Mesp2* expression patterns change cyclically at every somite formation, we initially tested whether those expression patterns change synchronously during somitogenesis. Bisected tail samples were subjected to in situ hybridization using *Mesp1* or *Mesp2* probes. As shown in Supplementary Fig. S4B, the expression levels of both signals do appear to change synchronously. Consequently, we speculated that the relative RNA levels for *Mesp1* and *Mesp2* could be analyzed using pooled RNA from several embryo samples. Subsequently, the value of *Mesp2* was normalized to *Mesp1* and we then compared the values during somitogenesis. As anticipated by the cyclic expression pattern, the value of *Mesp1* and *Mesp2* and the ratio between them revealed by the real-time PCR were varied even in the same developmental stage. However, we could confirm that the ratio became increased as somitogenesis progresses. The mean difference we have detected between E8.5 and E9.75 were 2.0-fold (Fig. 4C). These results suggest that the relative levels of *Mesp2* increase as somitogenesis proceeds, while the levels of *Mesp1* might be simultaneously reduced, in wild-type embryos.

Functional contributions of Mesp1 and Mesp2 during somitogenesis

Based on the above observations we hypothesized that (1) Mesp2 suppresses *Mesp1* expression in the later stage embryo, (2) the reduction of Mesp2 results in the de-repression of *Mesp1* and (3) a particular level of Mesp activity (Mesp1 + Mesp2) is required for the normal progression of somitogenesis (Figs. 4

Fig. 5. A working hypothesis for the skeletal phenotypes of the Mesp2-mutants, depicted in the right panels. By comparative analysis of *Mesp1* and *Mesp2* expression levels in the wild-type and mutant embryos, we speculate that the expression of *Mesp2* increases as somitogenesis progresses and that the levels of *Mesp1* are reduced in tandem in the wild-type embryo. A reduction of *Mesp2* function thus results in the de-repression of *Mesp1* expression. Somitogenesis proceeds normally when the functional levels of *Mesp1* and *Mesp2* are maintained above a specific threshold (indicated by the dotted line in the right panels). Green lines indicate abnormal skeletal regions. (A) In the wild-type embryo, normal skeletal formation is maintained by the collaborative expression and function of *Mesp1* and *Mesp2*. The levels of these two proteins are above the required functional threshold throughout somitogenesis. (B) In the P2-HD homozygous embryo, the collaborative activity of *Mesp1* and *Mesp2* is not sufficient to form the normal skeleton at the early stages of development since the level of P2-HD is low. However, the P2-HD expression increases in a manner similar to wild-type *Mesp2*, and the resulting Mesp activity reaches the required threshold at E9.5, which causes the restoration of normal somitogenesis thereafter. The skeletal defects are then restricted to the anterior half of the body, including the cervical and thoracic vertebrae, and the ribs. (C) In the presence of only a single P2-HD allele, there is some delay in the Mesp levels reaching their functional threshold (after E10.0), which results in the extension of the skeletal defects to the lumber vertebral level. (D) Further reduction of the *Mesp1* gene dosage compared with *Mesp2* HD/GFP causes a further extension of the defect into the sacral vertebrate. The collaborative activity of the Mesp gene reaches the required threshold at E10.5. (E) In the *Mesp2*-null mouse, *Mesp1* activity cannot reach the functional threshold during somitogenesis and the skeletal defects extend to the most posterior vertebra. (F) More severe defects are observed in the *Mesp2* GFP/dKO mouse, which has only a single *Mesp1* allele. The fetus thus shows severe truncation of the vertebra that might be due to the atrophy of somite derivatives. These data suggest that the relative contributions of *Mesp1* and *Mesp2* differ during somitogenesis.

and 5A), and skeletal defects will thus only be observed in the region where Mesp function is below this threshold level. According to this hypothesis, the phenotype of P2-HD can be interpreted as a lower Mesp activity (below the threshold) only in the early stage embryo (Fig. 5B). Since we do not know the definite values of *Mesp1* and *Mesp2* expression levels, we have arbitrarily defined the threshold level for Mesp activity in the wild-type embryo as the activity required for establishing normal rostro-caudal patterning, and we have assumed that only the relative ratios of Mesp1 and Mesp2 change during somitogenesis (Fig. 5A, right panel).

To evaluate our hypothesis, we genetically manipulated somitogenesis by changing the dosage of *Mesp1* and *Mesp2* and examining the resulting skeletal morphologies at E17.5. By

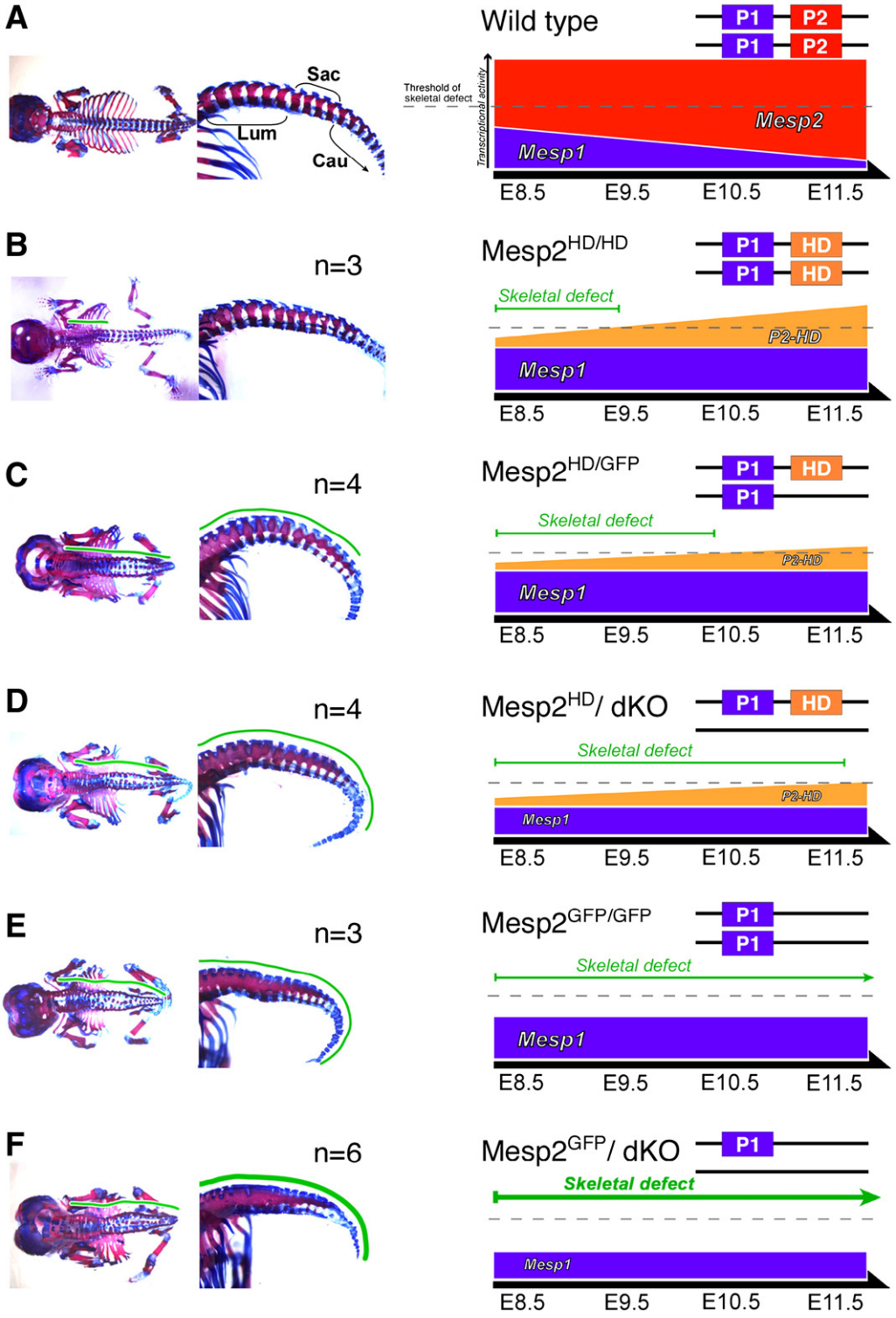

crossing P2-HD with either Mesp2 GFP or dKO mice we were able to compare the *Mesp1* dosage effects with the impact of a single *P2-HD* allele (Figs. 5C and D). At first, we found that the reduction of the P2-HD allele to a single dosage resulted in the extension of the skeletal defects in the posterior part of the body, which is visualized by the fusion of the pedicles of the neural arches (Fig. 5C, left panel). The Mesp2 HD/dKO mouse, which has both a single Mesp1 and P2-HD allele, showed a more posterior expansion of this defect; both the fusion of the pedicles and malformation of the caudal vertebra were evident (Fig. 5D, left panel). Mesp2 GFP/GFF (Mesp2-null) mice showed defects in their entire vertebra, and in this case we predict that the levels of Mesp1 will not reach the threshold level required for normal rostral–caudal patterning (Figs. 3B, 5E). The further reduction of Mesp1 levels in the Mesp2 GFP/dKO mouse resulted in the shortening of the trunk region, as well as more severe fusion of the vertebra (Fig. 5F). These phenotypes can be explained for each genotype by our current hypothesis (Fig. 5 right panel).

Discussion

Mesp2 protein stability is primarily regulated by a proteasome-mediated pathway

The most notable feature of the Mesp2 expression profile is the restriction of its expression domain in the anterior PSM, with a clear boundary formed that will demarcate the next segmental border (Morimoto et al., 2005). To establish the segmental boundary, at intervals of 2 h in mice, the protein would most likely need to be degraded once it achieves its function. In our current experiments, a molecular mapping study was successful in defining the "degradation domain" to amino acids 326–330 of the Mesp2 protein, which is required for proteolysis mediated by the proteasome in cultured cells (Fig. 1). However, the proteasome inhibitor MG132 did not completely abrogate Mesp2 proteolysis (Fig. 1B), indicating the involvement of additional proteolytic pathways in this regulation. We next attempted to determine the effects of this Mesp2 "degradation domain" in vivo by utilizing a knock-in strategy for the stabilized construct into the endogenous locus (Fig. 2). Unfortunately, however, this approach resulted in the reduction in the levels of transcription and we observed relatively severe defects in the control embryo into which a full-length Mesp2 fragment was introduced by a similar targeting strategy. These defects could be ascribed to the lower levels of expression of Mesp2 protein that are shown in Fig. 2B. In such a situation, a more highly stable Mesp2 variant might compensate for the lack of endogenous Mesp2 function. Thus we could not observe anomalies that were due to a more highly stabilized Mesp protein.

The P2-HD Mesp2 variant rescues the null defects in later stage embryos

We constructed a truncated Mesp2 protein composed of the NLS, bHLH and degradation domain, which we predicted would be the minimum requirements for a functional protein (Fig. S3C). The resulting knock-in mice displayed fused pedicles of the neural arches in both the cervical and thoracic regions (Fig. 3A), indicating that the somites were caudalized during the early stages of somitogenesis at E8.0–9.5 due to the lack of Mesp2 function. However, we could not detect any abnormalities in the expression pattern of *Uncx4.1*, which is a known downstream gene target of Mesp2 (Fig. 3B). This raised the interesting issue of why the region-specific defects of P2-HD occurred. The bHLH-type transcription factors are known to work as homo- or heterodimers via the binding to target gene enhancers. The targets may be selected by partnering factors and the transcriptional activity might then be determined by other interacting proteins recruited to the target sequences. In this regard, we have recently shown that Mesp2 forms a heterodimer with E47 and activates *EphA4* transcription via the binding of multiple E-boxes in the *EphA4* enhancer (Nakajima et al., 2006). It is possible that P2-HD may not have sufficient ability to recruit other transcription factors required for full activity. However, in the later stage embryo (after E9.5), the deficiencies of the P2-HD protein might be compensated for by increased levels of Mesp1, whereby Mesp function must reach a sufficient level to fulfill its functional role. Since the targets of Mesp2 that involved in pedicle formation have not yet been identified, other than *Uncx4.1*, it is not yet feasible to analyze the changes in the activity of these genes, the levels of which would be expected to be low in the early stages but sufficiently higher in the later stages of somitogenesis.

The gene dosage of Mesp1 and Mesp2 is critical for skeletal development

The *Mesp1* gene shows a similar expression pattern to *Mesp2* in the anterior PSM. In the Mesp2-null embryo, as well as in other knock-in mice in which Mesp2 function is expected to be reduced, the expression levels of *Mesp1* increase, indicating that Mesp2 generally suppresses *Mesp1* transcription. We have now found that the level of *Mesp2* expression increases as somitogenesis progresses, and that *Mesp1* expression consequently decreases during normal somitogenesis (Fig. 5A). In the P2-HD embryo, *Mesp1* expression was found to increase although it could not be determined whether this was because of the lower levels of P2-HD expression in our current knock-in strategy or due to the lesser ability of P2-HD to suppress *Mesp1* transcription. Unfortunately, we have no antibody to detect Mesp1 protein. Nevertheless, we speculate that P2-HD embryos can proceed with normal somitogenesis in the later stages of development because of the rescue of Mesp function by Mesp1 (Fig. 4). Since this compensatory phenomenon is mainly observed in later stage embryos, the dosage effect is detected from the anterior part and then spreads to the posterior region (Fig. 5).

The regulation of Mesp1 and Mesp2 during somitogenesis

Somitogenesis continues from stages E8.0 to E13.5 and the basic regulatory mechanisms underlying somite segmentation

are most likely similar but may have some variation during this process. It was recently shown in zebrafish that mutation of integrinα5 affects only the early stages of somitogenesis, although it is required for the maintenance of epithelial somites (Julich et al., 2005a; Koshida et al., 2005). The reverse phenomenon has been reported for mutants of Notch signaling pathway genes. In both zebrafish (Holley et al., 2002; Julich et al., 2005b) and mice (Conlon et al., 1995; Wong et al., 1997; Zhang and Gridley, 1998; Bessho et al., 2001), Notch signaling is involved in clock gene regulation and rostro-caudal patterning (Rida et al., 2004). In either case, the defects in Notch mutants become more severe as somitogenesis progresses. These data indicate that there could be some differences in the regulatory mechanisms along the A–P axis. These findings could also be explained by different contributions of similar factors or by specific developmentally regulated molecules. In the case of P2-HD homozygous mice, in which the defects are observed only in the anterior part of the axial skeleton (Figs. 3B and 5B), we do not think that the functions of Mesp1 and Mesp2 change during somitogenesis. We instead favor the idea that the levels of Mesp1 and Mesp2 change, and that a critical balance is maintained, during somitogenesis in the wild-type mouse.

Acknowledgments

We especially thank Yuki Takahashi for many technical supports and maintaining the mice used in this study. This work was supported by Grants-in-Aid for Science Research on Priority Areas (B), the Organized Research Combination System and National BioResource Project of the Ministry of Education, Culture, Sports, Science and Technology, Japan.

Appendix A. Supplementary data

Supplementary data associated with this article can be found, in the online version, at doi:10.1016/j.ydbio.2006.08.043.

References

Aulehla, A., Herrmann, B.G., 2004. Segmentation in vertebrates: clock and gradient finally joined. Genes Dev. 18, 2060–2067.

Aulehla, A., Johnson, R.L., 1999. Dynamic expression of lunatic fringe suggests a link between notch signaling and an autonomous cellular oscillator driving somite segmentation. Dev. Biol. 207, 49–61.

Aulehla, A., Wehrle, C., Brand-Saberi, B., Kemler, R., Gossler, A., Kanzler, B., Herrmann, B.G., 2003. Wnt3a plays a major role in the segmentation clock controlling somitogenesis. Dev. Cell 4, 395–406.

Bessho, Y., Sakata, R., Komatsu, S., Shiota, K., Yamada, S., Kageyama, R., 2001. Dynamic expression and essential functions of Hes7 in somite segmentation. Genes Dev. 15, 2642–2647.

Bessho, Y., Hirata, H., Masamizu, Y., Kageyama, R., 2003. Periodic repression by the bHLH factor Hes7 is an essential mechanism for the somite segmentation clock. Genes Dev. 17, 1451–1456.

Borycki, A.G., Emerson Jr., C.P., 2000. Multiple tissue interactions and signal transduction pathways control somite myogenesis. Curr. Top. Dev. Biol. 48, 165–224.

Brand-Saberi, B., Christ, B., 2000. Evolution and development of distinct cell lineages derived from somites. Curr. Top. Dev. Biol. 48, 1–42.

Conlon, R.A., Reaume, A.G., Rossant, J., 1995. Notch1 is required for the coordinate segmentation of somites. Development 121, 1533–1545.

Dubrulle, J., Pourquie, O., 2004. Coupling segmentation to axis formation. Development 131, 5783–5793.

Giudicelli, F., Lewis, J., 2004. The vertebrate segmentation clock. Curr. Opin. Genet. Dev. 14, 407–414.

Gossler, A., Tam, P.P.L., 2002. Somitogenesis: segmentation of the paraxial mesoderm and the delineation of tissue compartments. In: Rossant, J., Tam, P.P.L. (Eds.), Mouse Development. Academic Press, pp. 127–149.

Hirata, H., Bessho, Y., Kokubu, H., Masamizu, Y., Yamada, S., Lewis, J., Kageyama, R., 2004. Instability of Hes7 protein is crucial for the somite segmentation clock. Nat. Genet. 36, 750–754.

Holley, S.A., Julich, D., Rauch, G.J., Geisler, R., Nusslein-Volhard, C., 2002. her1 and the notch pathway function within the oscillator mechanism that regulates zebrafish somitogenesis. Development 129, 1175–1183.

Jouve, C., Palmeirim, I., Henrique, D., Beckers, J., Gossler, A., Ish-Horowicz, D., Pourquie, O., 2000. Notch signalling is required for cyclic expression of the hairy-like gene HES1 in the presomitic mesoderm. Development 127, 1421–1429.

Julich, D., Geisler, R., Holley, S.A., 2005a. Integrinalpha5 and delta/notch signaling have complementary spatiotemporal requirements during zebrafish somitogenesis. Dev. Cell 8, 575–586.

Julich, D., Hwee Lim, C., Round, J., Nicolaije, C., Schroeder, J., Davies, A., Geisler, R., Lewis, J., Jiang, Y.J., Holley, S.A., 2005b. beamter/deltaC and the role of Notch ligands in the zebrafish somite segmentation, hindbrain neurogenesis and hypochord differentiation. Dev. Biol. 286, 391–404.

Kitajima, S., Takagi, A., Inoue, T., Saga, Y., 2000. MesP1 and MesP2 are essential for the development of cardiac mesoderm. Development 127, 3215–3226.

Koshida, S., Kishimoto, Y., Ustumi, H., Shimizu, T., Furutani-Seiki, M., Kondoh, H., Takada, S., 2005. Integrinalpha5-dependent fibronectin accumulation for maintenance of somite boundaries in zebrafish embryos. Dev. Cell 8, 587–598.

Mansouri, A., Yokota, Y., Wehr, R., Copeland, N.G., Jenkins, N.A., Gruss, P., 1997. Paired-related murine homeobox gene expressed in the developing sclerotome, kidney, and nervous system. Dev. Dyn. 210, 53–65.

Monsoro-Burq, A.H., Le Douarin, N., 2000. Duality of molecular signaling involved in vertebral chondrogenesis. Curr. Top. Dev. Biol. 48, 43–75.

Morimoto, M., Takahashi, Y., Endo, M., Saga, Y., 2005. The Mesp2 transcription factor establishes segmental borders by suppressing Notch activity. Nature 435, 354–359.

Nakajima, Y., Morimoto, M., Takahashi, Y., Koseki, H., Saga, Y., 2006. Identification of Epha4 enhancer required for segmental expression and the regulation by Mesp2. Development 133, 2517–2525.

Pfaffl, M.W., 2001. A new mathematical model for relative quantification in real-time RT-PCR. Nucleic Acids Res. 29, e45.

Rida, P.C., Le Minh, N., Jiang, Y.J., 2004. A Notch feeling of somite segmentation and beyond. Dev. Biol. 265, 2–22.

Ririe, K.M., Rasmussen, R.P., Wittwer, C.T., 1997. Product differentiation by analysis of DNA melting curves during the polymerase chain reaction. Anal. Biochem. 245, 154–160.

Saga, Y., 1998. Genetic rescue of segmentation defect in MesP2-deficient mice by MesP1 gene replacement. Mech. Dev. 75, 53–66.

Saga, Y., Takeda, H., 2001. The making of the somite: molecular events in vertebrate segmentation. Nat. Rev., Genet. 2, 835–845.

Saga, Y., Hata, N., Koseki, H., Taketo, M.M., 1997. Mesp2: a novel mouse gene expressed in the presegmented mesoderm and essential for segmentation initiation. Genes Dev. 11, 1827–1839.

Saga, Y., Miyagawa-Tomita, S., Takagi, A., Kitajima, S., Miyazaki, J., Inoue, T., 1999. MesP1 is expressed in the heart precursor cells and required for the formation of a single heart tube. Development 126, 3437–3447.

Takahashi, Y., Koizumi, K., Takagi, A., Kitajima, S., Inoue, T., Koseki, H., Saga, Y., 2000. Mesp2 initiates somite segmentation through the Notch signalling pathway. Nat. Genet. 25, 390–396.

Takahashi, Y., Inoue, T., Gossler, A., Saga, Y., 2003. Feedback loops comprising

Dll1, Dll3 and Mesp2, and differential involvement of Psen1 are essential for rostrocaudal patterning of somites. Development 130, 4259–4268.

Takahashi, Y., Kitajima, S., Inoue, T., Kanno, J., Saga, Y., 2005. Differential contributions of Mesp1 and Mesp2 to the epithelialization and rostro-caudal patterning of somites. Development 132, 787–796.

Wong, P.C., Zheng, H., Chen, H., Becher, M.W., Sirinathsinghji, D.J., Trumbauer, M.E., Chen, H.Y., Price, D.L., Van der Ploeg, L.H., Sisodia, S.S., 1997. Presenilin 1 is required for Notch1 and DII1 expression in the paraxial mesoderm. Nature 387, 288–292.

Yagi, T., Tokunaga, T., Furuta, Y., Nada, S., Yoshida, M., Tsukada, T., Saga, Y., Takeda, N., Ikawa, Y., Aizawa, S., 1993. A novel ES cell line, TT2, with high germline-differentiating potency. Anal. Biochem. 214, 70–76.

Zhang, N., Gridley, T., 1998. Defects in somite formation in lunatic fringe-deficient mice. Nature 394, 374–377.